STIFFNESS MATRICES-BASED FORMALISM OF GROUND MOTION SYNTHESIS AND DIFFERENTIAL GROUND MOTIONS

Takanori HARADA[1] And Tsuneo OHSUMI[2]

SUMMARY

We will present the definition of the differential ground motions on free-field ground surface, and then describe numerical examples to show the characteristics of the differential ground motions as well as those of near-field ground motions. The differential ground motions and the ground motions in this paper are synthesised using a discrete three fold Fourier transform of the analytical forms of seismic wave field. They are derived by a stiffness matrices-based formulation of the physical processes of propagation of the seismic waves generated by a kinematic fault rupture model buried in horizontally layered media. In consequence, the differential ground motions and the ground motions in this paper can be synthesised in quite accuracy, because the seismic wave field in our method is represented as a simple sum of plane waves with the complex amplitudes given by the analytical forms in frequency wave number domain.

INTRODUCTION

Over the past 60 year of strong motion accelerograph development in seismic area, we have little data for strong ground motions in near earthquake faults, especially for differential ground motions, because the spacing between neighbouring accelerograph sites is usually much longer than the wavelengths of seismic waves. Consequently we know little about the characteristics of differential ground motions such as strains, tilts, and rotations as well as those of near-field strong ground motions. Dynamic deformations, equivalently, differential ground motions in near earthquake fault may play a major role in causing earthquake-related ground failure and damage to such extended structures as pipelines and long-span bridges. In this paper, we will present the definition of the differential ground motions on free-field ground surface, and then describe numerical examples to show the characteristics of the differential ground motions as well as those of near-field ground motions. The differential ground motions and the ground motions in this paper are synthesised using a discrete three fold Fourier transform of the analytical forms of seismic wave field. They are derived by a stiffness matrices-based formulation of the physical processes of propagation of the seismic waves generated by a kinematic fault rupture model buried in horizontally layered media. In consequence, the differential ground motions and the ground motions in this paper can be synthesised in quite accuracy, because the seismic wave field in our method is represented as a simple sum of plane waves with the complex amplitudes given by the analytical forms in frequency wave number domain.

DEFINITION OF DIFFERENTIAL GROUND MOTIONS

We will here summarise the definition and physical meanings of the differential ground motions on free-field ground surface, within the framework of the linear theory of elasticity. This means that the definition described in this paper is not applicable and must be redefined for the case where strains and displacements are relatively large. For such case, however, the definition in the frameworks of linear theory of elasticity may still be used as a measure of the degree of the ground failure as well as the degree of the spatial variation of ground motions.

We denote the three displacement components at a position (x, y, z) of a time instant t in the Cartesian coordinate system by $u(x, y, z, t)$, $v(x, y, z, t)$, and $w(x, y, z, t)$. Then, the small angle of rotation about axes parallel to x, y, and z are given as [Chou *et al.*, 1967],

[1]   Dept of Civil and Environmental Engineering, Miyazaki University, Japan Email:harada@civil.miyazaki-u.ac.jp
[2]   Planning and Research Department, Nippon Koei,Co.,Ltd,, Ibaraki, Japan, Email:a3850@n-koei.co.jp

1. $$\omega_x = \frac{1}{2}\left(\frac{\partial w}{\partial y} - \frac{\partial v}{\partial z}\right), \quad \omega_y = \frac{1}{2}\left(\frac{\partial u}{\partial z} - \frac{\partial w}{\partial x}\right), \quad \omega_z = \frac{1}{2}\left(\frac{\partial v}{\partial x} - \frac{\partial u}{\partial y}\right) \tag{1}$$

in which each of these three rotational components is positive if counter-clockwise when viewed from the positive extension of the axis of rotation toward the origin.

On the free-field ground surface, the stresses must be zero. Accordingly, such relations must exist on the free-field ground surface as,

$$\frac{\partial u}{\partial z} = -\frac{\partial w}{\partial x}, \quad \frac{\partial v}{\partial x} = -\frac{\partial w}{\partial z}, \quad \frac{\partial w}{\partial x} = -\frac{\lambda}{\lambda + 2\mu}\left(\frac{\partial u}{\partial x} + \frac{\partial v}{\partial y}\right) \tag{2}$$

where λ and μ are Lame's constants.

Therefore, substituting Eq.(2) into Eq.(1), the expression of the rotational components on free-field ground surface are given by

$$\omega_x(x,y,t) = \frac{\partial w}{\partial y}, \quad \omega_y(x,y,t) = -\frac{\partial w}{\partial x}, \quad \omega_z(x,y,t) = \frac{1}{2}\left(\frac{\partial v}{\partial x} - \frac{\partial u}{\partial y}\right) \tag{3}$$

where u, v, and w are the displacements on the free-field ground surface.

Next we will summarise the expressions for the six components of free-field ground surface strains. It is well known that the longitudinal components of strains are given by

$$\varepsilon_{xx}(x,y,t) = \frac{\partial u}{\partial x}, \quad \varepsilon_{yy}(x,y,t) = \frac{\partial v}{\partial y} \tag{4}$$

By taking an average of the longitudinal strains, the dilatational component of strain is obtained as

$$\varepsilon_D(x,y,t) = \frac{1}{2}\left(\frac{\partial u}{\partial x} + \frac{\partial v}{\partial y}\right) \tag{5}$$

The components of pure shear strains in x, and y directions, respectively, are expressed as

$$\gamma_x(x,y,t) = \frac{\partial u}{\partial y}, \quad \gamma_y(x,y,t) = \frac{\partial v}{\partial x} \tag{6}$$

Taking an average of the pure shear strains yields the shear strain on x-y plane which corresponds to the free-field ground surface,

$$\gamma_{xy}(x,y,t) = \frac{1}{2}\left(\frac{\partial u}{\partial y} + \frac{\partial v}{\partial x}\right) \tag{7}$$

In the next paragraphs we will describes the physical meanings of the rotation ω_z about z axis and the dilatational strain ε_D given by Eq(3) and Eq(5), in relation to such seismic waves as SH and P-SV waves.

For the axis-symmetrical case where the material and structural properties of the earth medium through which the seismic waves propagate are axis-symmetrical, the displacements $u(x,y,z,t)$, $v(x,y,z,t)$, and $w(x,y,z,t)$ are composed by the following equations,

$$u = u_0\cos\theta - v_0\sin\theta, \quad v = u_0\sin\theta + v_0\cos\theta, \quad w = w_0 \tag{8}$$

where $u_0(x',z,t)$ and $w_0(x',z,t)$ are the out-plane wave displacements created by the P and SV waves , and the out-plane wave displacement is expressed by $v_0(x',z,t)$ generated by the SH wave alone. In the above equations, the direction of the P-SV and SH waves is assumed to be toward x' axis and lie in the same vertical x'-z plane which is obtained by a rotation with angle θ about the vertical axis . Accordingly, the original coordinates x,y, and z are related to the rotated new coordinates x',y', and z by the following equations,

$$x' = x\cos\theta + y\sin\theta , \quad y' = x\sin\theta + y\cos\theta , \quad z' = z \tag{9}$$

Substitution of Eq.(8) into Eq.(3) and Eq.(5) by considering Eq.(9) yields

$$\omega_z(x,y,t) = \frac{1}{2}\left(\frac{\partial v}{\partial x} - \frac{\partial u}{\partial y}\right) = \frac{1}{2}\frac{\partial v_0}{\partial x'} , \quad \varepsilon_D(x,y,t) = \frac{1}{2}\left(\frac{\partial u}{\partial x} - \frac{\partial v}{\partial y}\right) = \frac{1}{2}\frac{\partial u_0}{\partial x'} \tag{10}$$

It is observed from above equations that the rotation ω_z about the vertical axis z on free-field ground surface is associated with the pure shear strain in the y' direction, which is generated by the SH wave alone, while the dilatational strain ε_D is the axial strain in the x' direction generetaed by the P-SV waves. This physical meanings of ω_z and ε_D was applied to the decomposition of the observed seismograms into the SH and P-SV wave compoments [Sato, 1968].

STIFFNESS MATRICES-BASED FORMULATION OF GROUND MOTIONS

The starting equation is the following stiffness matrix equation for a horizontal layer, which includes an extended rupturing fault, as shown in Figure 1.
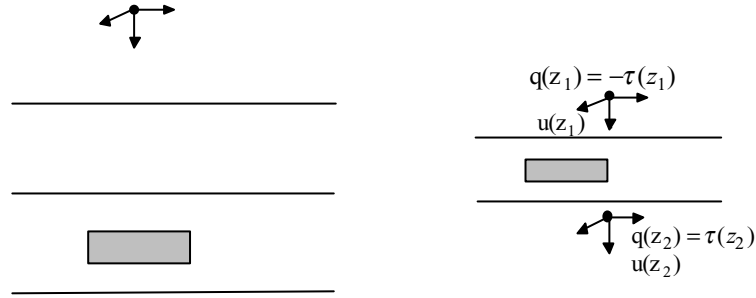
Figure 1:A horizontal layered system including an extended rupturing fault

$$\begin{pmatrix} \mathbf{q}(z_1) + \mathbf{q}_s(z_1) \\ \mathbf{q}(z_2) + \mathbf{q}_s(z_2) \end{pmatrix} = \begin{pmatrix} \mathbf{K}_{11}^{(2)} & \mathbf{K}_{12}^{(2)} \\ \mathbf{K}_{21}^{(2)} & \mathbf{K}_{22}^{(2)} \end{pmatrix} \begin{pmatrix} \mathbf{u}(z_1) \\ \mathbf{u}(z_2) \end{pmatrix} \tag{11a}$$

where,

$$\begin{pmatrix} \mathbf{q}_s(z_1) \\ \mathbf{q}_s(z_2) \end{pmatrix} = \begin{pmatrix} \mathbf{K}_{11}^{(2)} & \mathbf{K}_{12}^{(2)} \\ \mathbf{K}_{21}^{(2)} & \mathbf{K}_{22}^{(2)} \end{pmatrix} \begin{pmatrix} \mathbf{u}_s(z_1) \\ \mathbf{u}_s(z_2) \end{pmatrix} - \begin{pmatrix} -\tau_s(z_1) \\ \tau_s(z_2) \end{pmatrix} \tag{11b}$$

In Eq.(11a), $q(z_1)$= $\tau(z_1)$ and $q(z_2)$= $\tau(z_2)$. $u(z_j)$ and $\tau(z_j)$ are the displacement and stress vectors at a depth z_j in frequency wave number domain, and also $K^{(2)}{}_{ij}$ is the element stiffness matrix in frequency wave number domain [Harada et al., 1999]. In Eq.(11b), $u_s(z_j)$ and $\tau_s(z_j)$ are the displacement and stress vectors at a depth z_j, created by the extended rupturing fault buried in full space. For a half space including the extended rupturing fault, it is obtained in a similar manner such as,

$$q(z_2) + q_s(z_2) = K_{Half}u(z_2) , \quad q_s(z_2) = K_{Half}u_{free}(z_2) \tag{12}$$

where $\boldsymbol{K}_{half}$ is the stiffness matrix for a half space, and $\boldsymbol{u}_{free}(z_2)$ is the free-field surface displacement of the half space, which is generated by the extended rupturing fault. The closed form expressions for the element stiffness matrix $\boldsymbol{K}^{(2)}{}_{ij}$, $\boldsymbol{K}_{half}$, $\boldsymbol{u}_s(z_j)$, $\boldsymbol{\tau}_s(z_j)$, and $\boldsymbol{u}_{free}(z_2)$ are presented in the paper [Harada , et al., 1999].

It is well known in structural analysis that the system stiffness matrix equation for a two horizontal layered media overlying a half space as shown in Figure 1, where an extended rupturing fault is included in the 2nd layer, can be easily obtained, using a direct superposition technique of the element stiffness matrix given by Eq.(11), such as,

$$\begin{pmatrix} \boldsymbol{K}_{11}^{(1)} & \boldsymbol{K}_{12}^{(1)} & \\ \boldsymbol{K}_{21}^{(1)} & \boldsymbol{K}_{22}^{(1)}+\boldsymbol{K}_{11}^{(2)} & \boldsymbol{K}_{12}^{(2)} \\ & \boldsymbol{K}_{21}^{(2)} & \boldsymbol{K}_{22}^{(2)}+\boldsymbol{K}_{Half} \end{pmatrix}\begin{pmatrix} \boldsymbol{u}(z_0) \\ \boldsymbol{u}(z_1) \\ \boldsymbol{u}(z_2) \end{pmatrix}=\begin{pmatrix} 0 \\ \boldsymbol{q}_s(z_1) \\ \boldsymbol{q}_s(z_2) \end{pmatrix} \tag{13}$$

By solving the above system equation, the free-field ground surface displacement $\boldsymbol{u}(z_0)=\boldsymbol{u}(k_x,k_y,\omega)$ in frequency wave number domain is obtained. Then the free-field ground surface displacement $\boldsymbol{u}(x,y,t)$ in space time domain can be computed by the three fold Fourier transform such as,

$$\boldsymbol{u}(x,y,t)=\frac{1}{(2\pi)^3}\iiint \boldsymbol{u}(\kappa_x,\kappa_y,\omega)e^{i[\kappa_x x+\kappa_y y-\omega t]}d\kappa_x d\kappa_y d\omega \tag{14}$$

where $\boldsymbol{u}(x,y,t)$ is the displacement vector in the space-time domain with components $(u(x,y,t), v(x,y,t), w(x,y,t))$, and $\boldsymbol{u}(z_0)=\boldsymbol{u}(k_x, k_y, \omega)$ is the displacement vector in the frequency wave number domain with components $(u(k_x, k_y, \omega), v(k_x, k_y, \omega), w(k_x, k_y, \omega))$, which is a function of not only the wave numbers k_x, and k_y in the directions of x, and y axses, respectively, but also the frequency ω. On the basis of the stiffness matrices formulation, the closed form analytical expressions of $\boldsymbol{u}(k_x, k_y, \omega)$ are described for the multiple horizontal earth layers over the half space media in which a rupturing rectangular fault is buried[Harada et al., 1999].

The above three fold Fourier transform can be computed efficiently by using the discrete FFT (Fast Fourier Transform) algorithm with the following discretization parameters,

$$\Delta\omega=\frac{\omega_{max}}{N_\omega}, \Delta\kappa_x=\frac{\kappa_{x max}}{N_\kappa}, \Delta\kappa_y=\frac{\kappa_{y max}}{N_\kappa}, \Delta t=\frac{2\pi}{2\omega_{max}}, \Delta x=\frac{2\pi}{2\kappa_{x max}}, \Delta y=\frac{2\pi}{2\kappa_{y max}} \tag{15}$$

where ω_{max}, κ_{xmax} and κ_{ymax} represent the upper cut-off frequency and wave number, $|\omega|<\omega_{max}$, $|\kappa_x|<\kappa_{xmax}$, $|\kappa_y|<k_{ymax}$, beyond which the complex displacement amplitude $\boldsymbol{u}(k_x,k_y,\omega)$ of plane wave may be assumed to be zero for either mathematical or physical reasons.

NUMERICAL EXAMPLE OF SYNTHESIS OF NEAR-FIELD GROUND MOTIONS-1966 PARKFIELD EARTHQUAKE GROUND MOTIONS-

We synthesised the station 2 motions by using the fault-medium model of Bouchon (1979) where the source is a single vertical rectangular strike slip fault with the rupture velocity of 2.2 km/s, and the earth medium consists of a sedimentary horizontal layer with the thickness of 1.5 km overlying a half space in which the fault is buried. The detailed fault parameters used in this study are indicated in Table 1.

Table 1: Source parameters		Table 2: Discretization parameters	
Seismic Moment	$M_0 = 2.230 \times 10^{17}$ N·m	Cutoff frequency ω_{max} (rad/sec)	12.0
	(2.230×10^{24} dyne·cm)	Cutoff x-wavenumber k_{xmax} (rad/m)	4.0×10^{-3}
Rise Time of the Ramp Function	$T = 0.3$ sec	Cutoff y-wavenumber k_{ymax} (rad/m)	4.0×10^{-3}
Length of Fault	$L = 8500$ m	$N_{f\omega}$	256
Width of Fault	$W = 8500$ m	N_{fk}	256
Velocity of Rupture	$v_r = 2200$ m/sec	Δt (sec)	0.262
Depth of Upper Edge of Fault	$z_{so} = 0$ m	Δx (m)	785
Strike Angle	$\phi = 0°$	Δy (m)	785
Dip Angle	$\delta = 90°$		
Slip Angle	$\lambda = 0°$		
Slip Type	Type 1		

(a) Observed transverse ground motion displacement, velocity, and acceleration in frequency up to 2.0 Hz at station 2 during the 1966 Parkfield earthquake
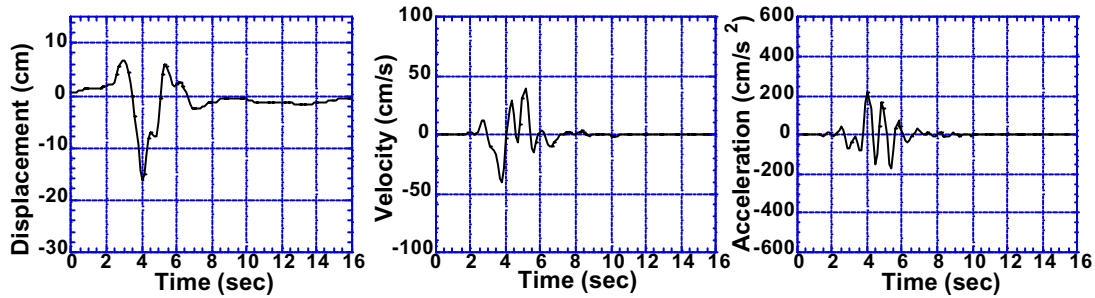
(b) Synthesized transverse ground motion displacement, velocity, and acceleration in frequency up to 2.0 Hz at station 2 using the Bouchon source-medium model
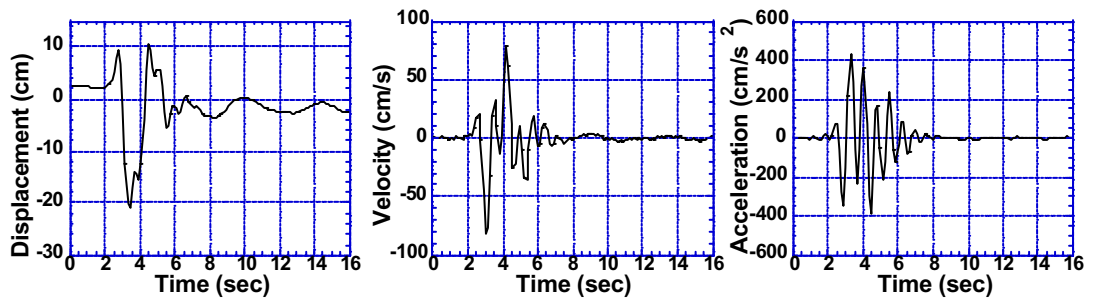
(c) Synthesized transverse ground motion displacement, velocity, and acceleration in frequency up to 2.0 Hz at station 2 using the modified Bouchon source-medium model

Figure 2: Comparison of the observed records with the   synthesized ground motions from the two source-medium models
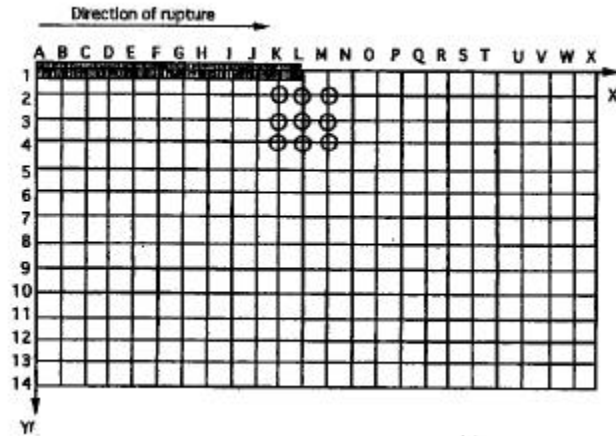
Figure 3: Near-field ground surface and projected fault location used in computation
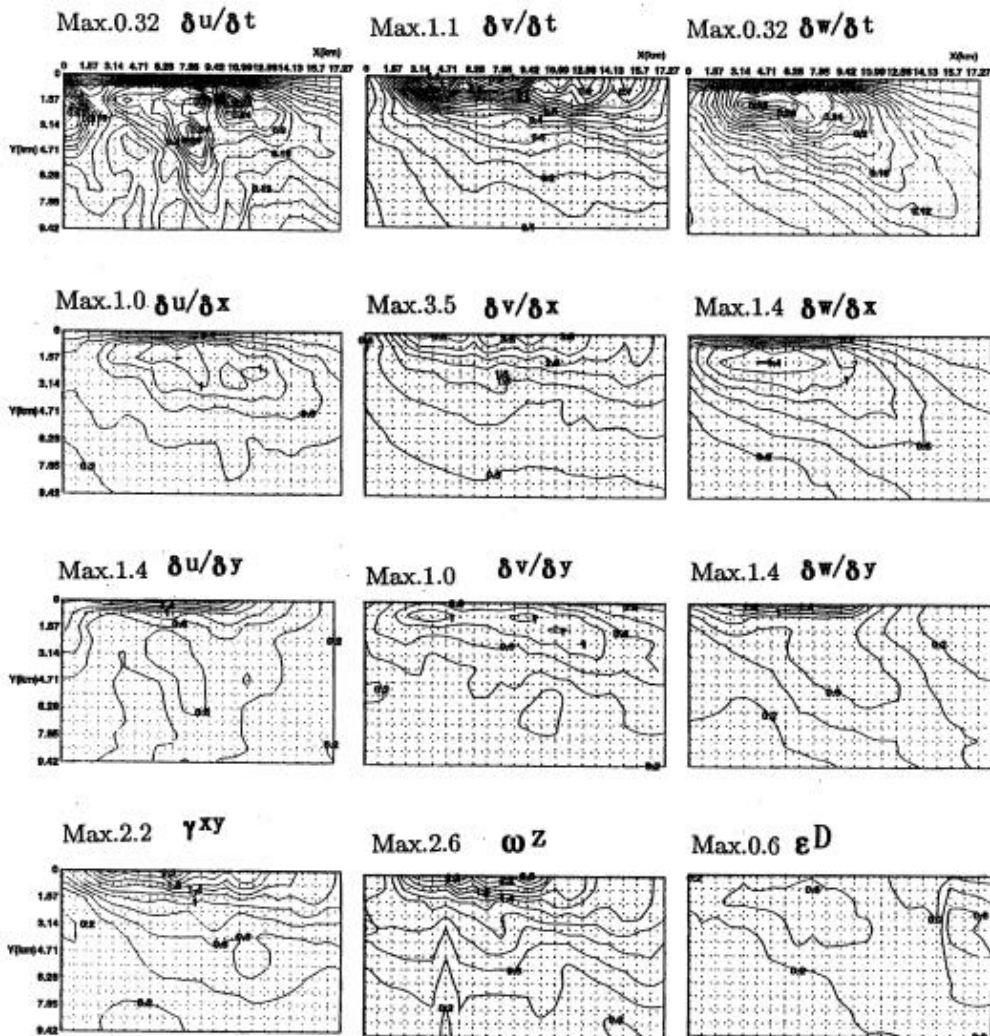
Figure 4:Spatial variation of maximum values of synthesised 3 components of ground velocities and of 9 components of differential ground motions
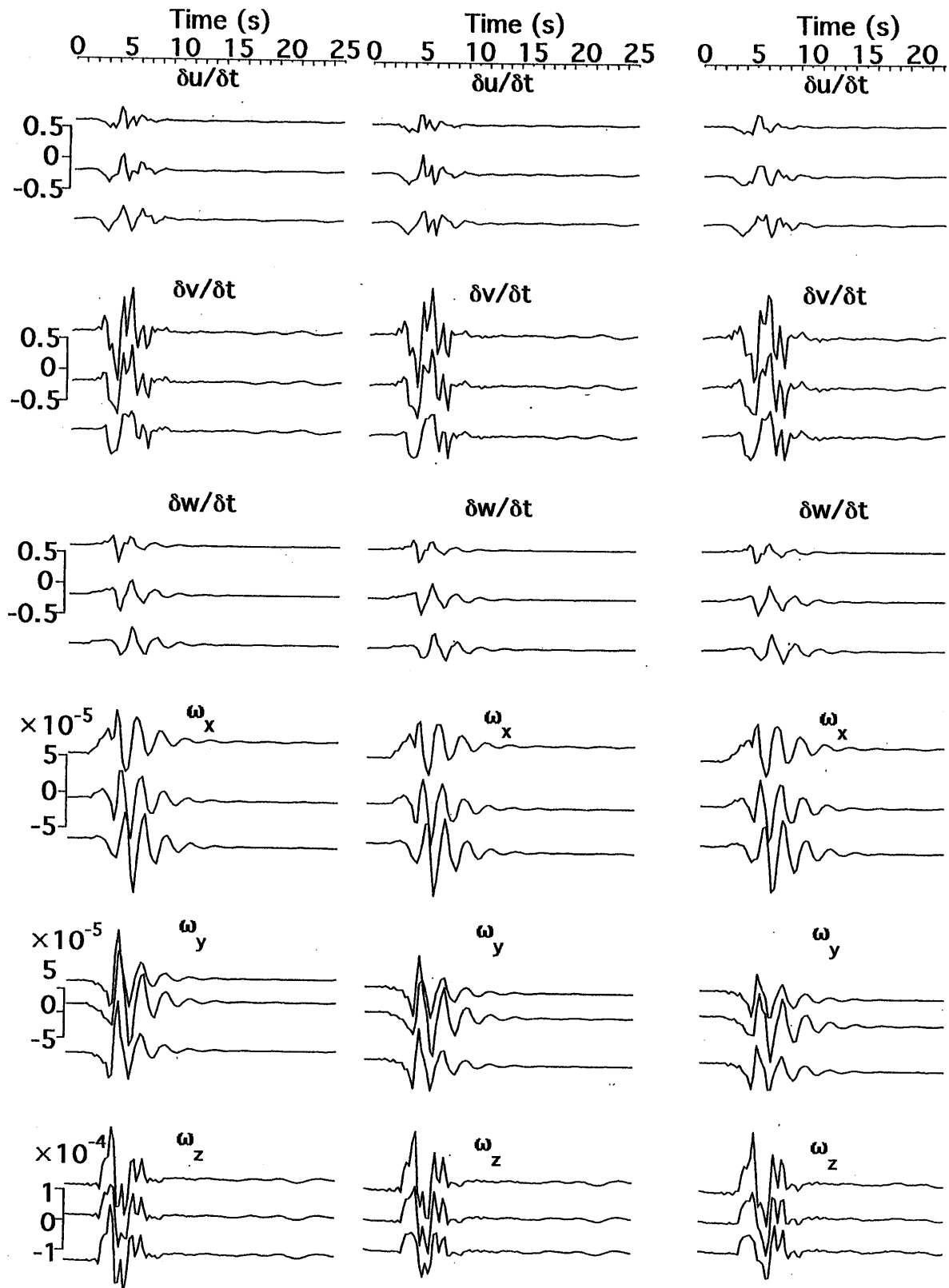
Figure 5: Time histories of synthesised 3 components of ground velocities and of 3 components of rotational ground motions at nine sites indicated by circles in Figure 3

The discretization parameters used in this synthesis are also indicated in Table 2. The earth medium properties necessary for the synthesis are: for a sedimentary layer, the thickness = 1.5 km, the S wave speed =1.6 km/s, the P wave speed =2.8 km/s, the density = 2.3 t/m^3, and the Q value =150, for the half space, the S wave speed =3.5 km/s, the P wave speed =6.0 km/s, the density = 2.8 t/m^3, and the Q value =400.

For the above described Bouchon model, the synthesised ground motion displacement, velocity, and acceleration time histories in frequency up to 2 Hz are shown in Figure 2(b), by comparing the observed ground motion time histories in frequency up to 2 Hz. In this synthesis the average slip displacement D is assumed to be 50 cm. It is observed from Figure 2(a) and (b) that the detailed wave forms, especially for the velocity and acceleration time histories, are different from the observed records, although gross wave forms are similar to the observed records.

To improve such above inconsistency of detail wave forms, we investigated the effect of the parameters on the wave forms. Finally we have obtained the relatively nice results in wave forms as shown in Figure2(c) by changing only the values of thickness of sedimentary layer and fault rupture speed from the original values of 1.5 km and 2.2 km/s to 1.0 km and 2.75 km/s. Such values may be within the range of available possibility.

NUMERICAL EXAMPLE OF SYNTHESIS OF DIFFRENTIAL DROUND MOTIONS

By using the fault-medium model of Bouchon (1979) which is shown in previous chapter 4, we synthesised nine components of differential ground motions defined in chapter 2. Figure 3 shows the free-field ground surface area and the projection of the vertical strike fault to the ground surface used in this analysis.

Figure 4 shows the spatial variation of the maximum values of three components of ground velocities and of nine components of differential ground motions on the near-field area as shown in Figure 3. It is observed from Figure 3 that the differential motions($\partial u/\partial x, \partial v/\partial x, \partial w/\partial x$) may be obtained from the ground velocities, dividing them by the fault rupture velocity (in this case 2.2km/s). It is also observed that the wave field may be controlled by the SH wave (Love wave) because the maximum value of ω_z is quite larger than that of ε_D (see chapter 2). Figure 5 shows the time histories of three components of ground velocities and of 3 rotational components ω_x, ω_y, ω_z at nine sites near the fault end area as indicated by circles in Figure 3. It is observed from Figure 5 that the larger amplitude pulse waves appear in the ground velocities transeverse to the fault.

The characteristics of the differential ground motions as well as ground motions shown in Figures 4 and 5 may influence on the ground failure and the damage to the extended strucures such as pipelines and long-span bridges. Untill now, we have little data for strong ground motions in near earthquake faults, especially for differential ground motions. Accordingly, the effects of them on the structural responses have not been sufficiently investigated so far. The study on such relations between the structural damages and the ground motions, especially the differential ground motions should be necessary.

REFERENCES

Bouchon, M. (1979) Predictability of ground displacement and velocity near an earthquake fault: An example: The Parkfield earthquake of 1966, *Journal of Geophysical Research*, Vol. 84, No.B11, pp.6149-6156 .
Chou,P.C.(1967) *Elasticity*, Van Nostrand Company.
Harada,T., Ohsumi,T., and Okukura,H.(1999) Analytical solutions of wave field in 3-dimensional Cartesian coordinate and their application to synthesis of seismic ground motions, *Journal of Japan Society of Civil Engineers*, in Japanese, No.612/I-46, pp.99-108.
Saito,M.(1968) Synthesis of rotational and dilatational seismograms, *Journal of Physics of Earth*, Vol.16,pp.53-62